



A Common Capacitor Hybrid Buck-Boost Converter

Erol Can* 

Department of Aviation Electrical and Electronics, School of Civil Aviation, Erzincan Binali Yildirim University,
Erzincan, Turkey
E-mail: ccn_e@hotmail.com

Received: October 24, 2022

Revised: November 28, 2022

Accepted: December 1, 2022

Abstract— DC-DC converters are electronic circuit elements that are frequently used to change the direct current (DC) level. This paper presents a hybrid buck-boost converter - with constant modulation index - that can change a DC voltage at two directions compared to the conventional buck-boost DC-DC converters. First, the circuit structure and operation are given. Then, the performance of the proposed converter is tested on resistive and inductive loads, and compared with that of conventional buck-boost converters. The obtained results demonstrate the effectiveness of the proposed converter. They unveil that the proposed converter - compared to the conventional buck-boost converters - produces a higher and flexible rate of conversion without changing the operating ratio of the switches. Moreover, the proposed converter is able to change the voltage on double way on load for a constant operating ratio, while the traditional converters provide a one-way conversion.

Keywords— Hybrid buck-boost converter; Conversion rate; Flexible rate.

1. INTRODUCTION

Photovoltaic (PV) energy systems are examples of systems that produce direct current (DC) [1-3]. At the output of such energy generation systems, DC-DC converters can be used in order to increase and decrease the electrical energy to change it to the desired level [4-7]. Also, the need for controllable electrical power has increased rapidly with the rapid development of the industry. DC-DC converters are considered for important industrial power electronics applications such as uninterruptible power supplies (UPS), battery chargers, switched DC/DC power supplies and static voltage regulators [8-10]. Conventional converters with one-way conversion can operate only as incrementing or simply decrementing with an operating ratio between 0-1 [11-14]. On the other hand, DC-DC converters with bidirectional operation can operate in decreasing and increasing modes between 0-0.5 and 0.5-1 of operating ratios [15, 16]. A circuit structure that can use the 0-1 operating ratio - in both increasing and decreasing mode in order to achieve more flexible and wide-range electrical energy conversion in applications - will provide an operating advantage for power systems. Therefore, the design and application of the hybrid buck-boost converter is presented in this study. In the proposed system, buck and boost converters provide energy to the load through a common capacitor. Unlike the traditional buck-boost converters, the operating ratios of the proposed converter switches are not changed between 0-1. Switches and diodes added to the converter structures are activated sequentially by a second pulse width modulation (PWM) generator, providing bidirectional energy level

* Corresponding author

changes on the load without changing the operating ratios of the power switches. The structure, operation and properties of the proposed converter circuit are given with mathematical explanations in section 2. In the section 3, the operation and performance of the circuit are tested in MATLAB Simulink for different loads that are resistive (R) load and resistive and inductive (RL) loads, and measurements and observations are made. The results obtained with the proposed method are compared with the results obtained with the traditional methods by making current-voltage measurements on the loads in section 4. Section 5 gives the conclusions.

2. HYBRID BUCK-BOOST CONVERTER

The hybrid buck-boost converter circuit structure is given in Fig. 1. There are four power switches from S_1 to S_4 on the circuit, three diodes from D_1 to D_3 , two inductors from L_1 to L_2 , two sources from V_{dc1} to V_{dc2} and a capacitor as C .

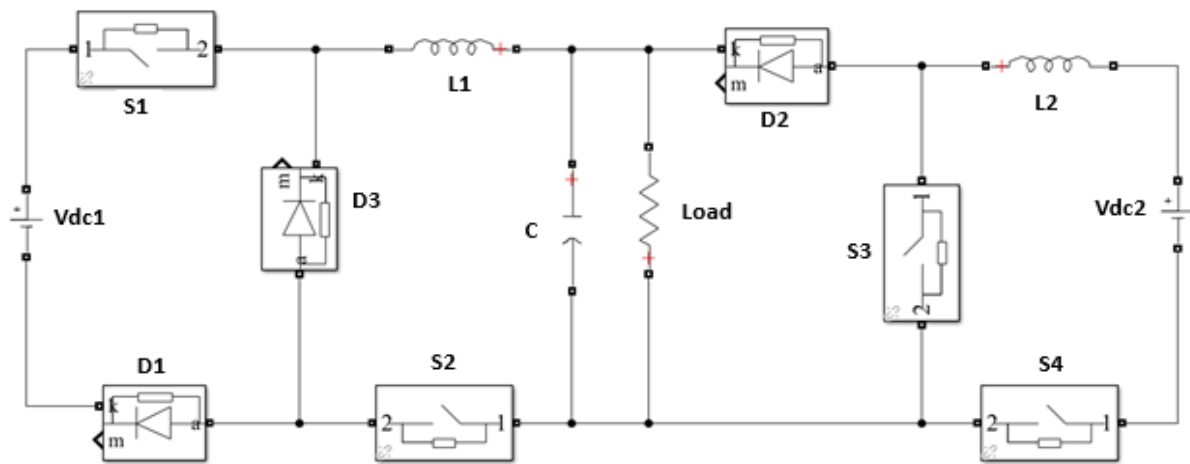


Fig. 1. The proposed hybrid buck-boost converter.

The lossless step-up DC-DC converter circuit studied in continuous conduction is shown in Fig. 2. The operating current and voltage waveforms are shown in Fig. 3. D is the swing ratio of the power switches and takes a value between 0 and 1, multiplied by T to be expressed as time. The operation of the circuit is divided into two modes: the first mode is in the range $0 < DT < T < t_1$ and it is shown in Fig. 2(a) for the time $0-DT$. During this mode, the S_1 , S_2 switches and the D_1 diode is on, while the D_3 diode is blocking. The main task of the D_3 diode is to prevent leaks from the other source when the combined hybrid buck-boost converter switches from decreasing mode to boosting mode. As given in Fig. 3(a), the voltage on L_1 is $V_{dc}-V_c$ and the current I_{L1} reaches maximum values. The other mode occurs in the range $0 < (1-D)T < T < t_1$ and is shown in Fig. 2(b). During this mode, S_1 is in switch blocking and diode D_3 is conducting. In this operating mode of the circuit, as given in Fig. 3(a), the voltage $-V_c$ and current I_{L1} on L_1 reach their minimum values. V_c is also the output voltage as V_o . The voltage value formed for this process can be expressed as follows.

$$\frac{V_o}{V_{dc1}} = D \cdot t_1 \quad (1)$$

$$V_o = V_{dc1} D \cdot t_1 \quad (2)$$

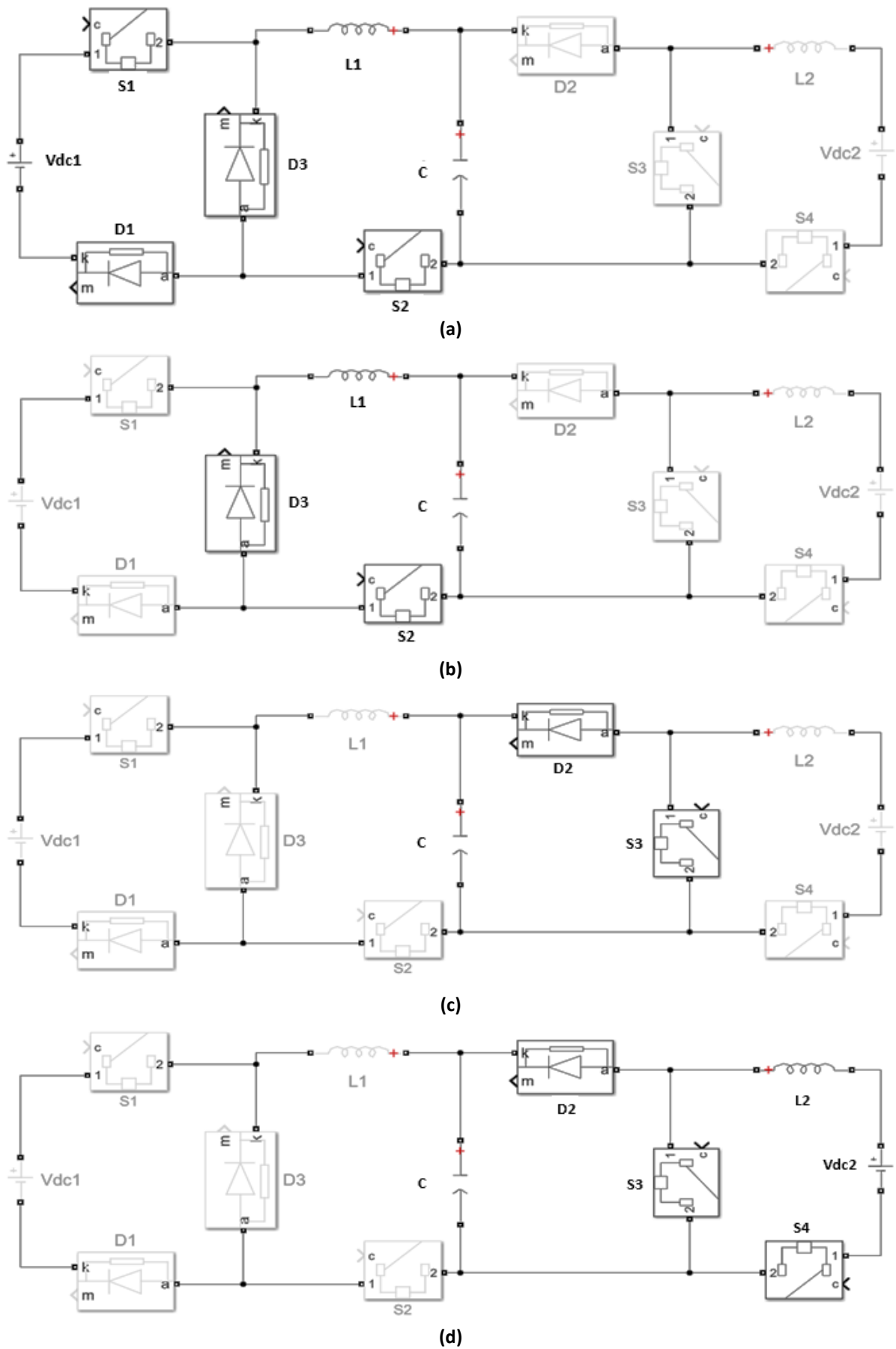


Fig. 2. a) buck mode at DT ; b) buck mode at $(1-D)T$; c) boost mode at DT ; d) boost mode at $(1-D)T$ of the proposed hybrid buck-boost converter:

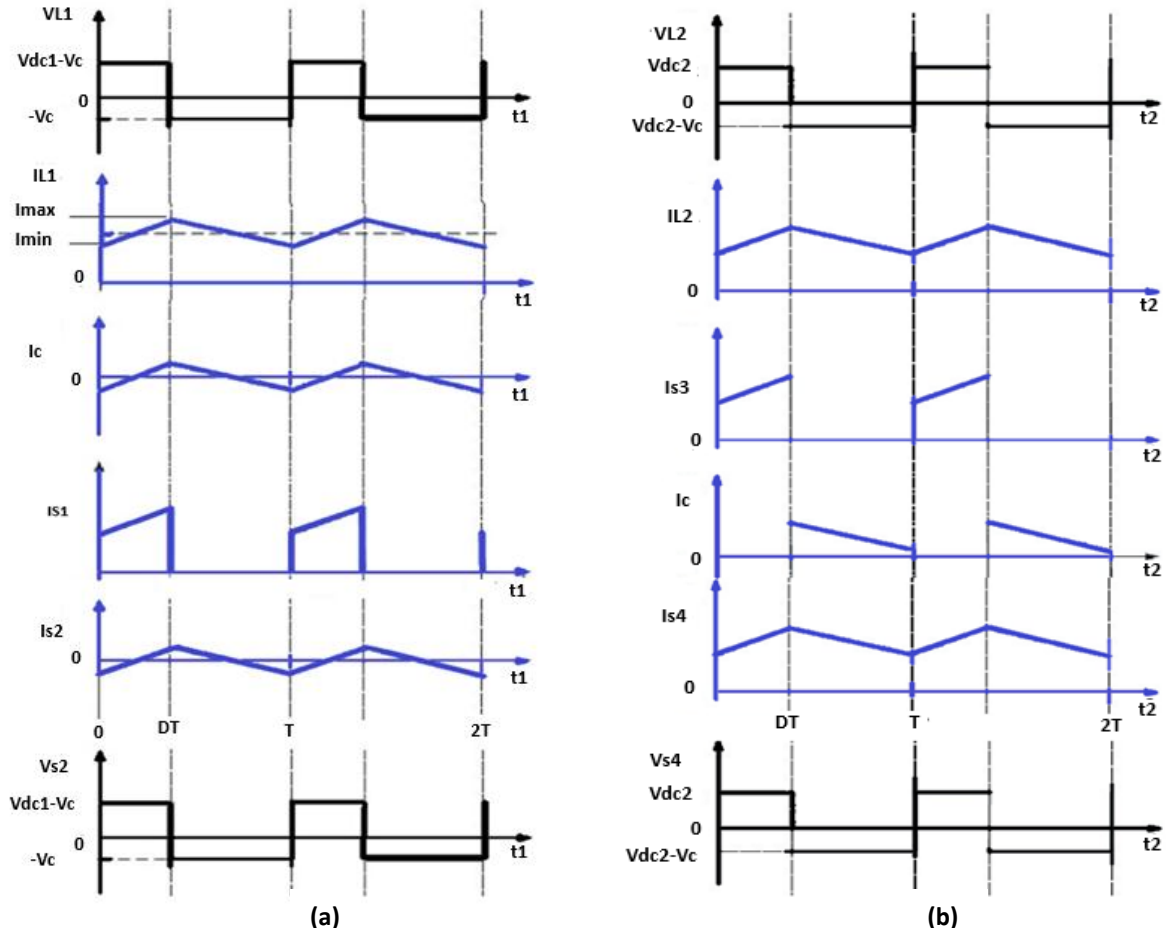


Fig. 3. Operating current and voltage waveforms: a) buck mode at t1; b) boost mode at t2.

In the increasing mode, while the working rates are the same, a second total working time is given as t_2 . When $k \in \mathbb{Z}^+$ $k = \{1, 2, 3, \dots, \infty\}$, t can be calculated as follows if the running time of the circuit is expressed as t .

$$t = t_1 + t_2 \tag{3}$$

$$t_1 = kt_2 \tag{4}$$

The operation of the circuit in the second stage is also divided into two modes: the first mode is in the range $0 < DT < T < t_2$ and is shown in Fig. 2(c) for the time $0-DT$. Switches S_3 and S_4 are on during this mode. The main task of the D_4 diode is to prevent leaks from the other source when the combined hybrid buck-boost converter switches from reducing mode to boosting mode. As shown in Fig. 3(b), the voltage V_{dc} on L_2 and the current I_{L1} reach their maximum values. The other mode occurs in the range $0 < (1-D)T < T < t_2$ and is shown in Fig. 2(d). During this mode, S_3 is in switch blocking and diode D_2 is conducting. In this operating mode, as given in Fig. 3(b), the voltage on L_1 ($V_{dc2}-V_c$) and the current I_{L1} reach their minimum values. V_c is also the output voltage as V_o . The voltage value formed for this process can be expressed as follows:

$$\frac{V_o}{V_{dc2}} = \frac{t_2}{(1-D)} \tag{5}$$

$$V_o = \frac{V_{dc2} \cdot t_2}{(1-D)} \tag{6}$$

When $V_{dc2}=V_{dc1}=V_{dc}$, the multiplicity mean value for the total time t can be calculated as:

$$V_o = \left[V_{dc} D \cdot t_1 + \frac{V_{dc} \cdot t_2}{(1-D)} \right] / (t_1 + t_2) \quad (7)$$

$$V_o = \left[V_{dc} D \cdot k t_2 + \frac{V_{dc} \cdot t_2}{(1-D)} \right] / (k t_2 + t_2) \quad (8)$$

$$V_o = \left[V_{dc} D \cdot k + \frac{V_{dc}}{(1-D)} \right] / (k + 1) \quad (9)$$

Power converters have losses due to the operating characteristics of the circuit elements. In order to specify the circuit characteristics and efficiency in DC-DC converter circuit design, mathematical expressions that give the relationship between circuit losses, output power and efficiency are very important in terms of describing the presented system [17-19]. When the sum of these losses is added to the power obtained at the output, it expresses the total power of the circuit. The ratio of the total power to the power obtained at the output of the circuit constitutes the efficiency of the stream. The calculation of the losses of the power elements is made by considering the methods suggested in [20, 21]. The conduction loss caused by the resistor is $P_{on,h}$, $P_{on,l}$ depending on whether the used MOSFET power switch is on or off. The switching losses of the MOSFET are P_{s-h} , P_{s-l} . The recovery loss of the diode is P_{di} . The conduction loss in the inductor is P_{Lr} . The loss in the capacitor is P_{CA} and I_o is output current, R_{on-h} is high-side on-resistance for MOSFET, R_{on-l} is low-side on-resistance for MOSFET, V_{dc} is input voltage, V_o is output voltage. The main conduction losses for the position of the power switch being connected directly to the source with no load in between are found as follows:

$$P_{on-h} = I_o^2 \times R_{on-l} \times V_o / V_{dc} \quad (10)$$

If there is a load between the power switch and the source, this time the conduction loss is found as in Eq. (11).

$$P_{on-l} = I_o^2 \times R_{on-h} \times [1 - (V_o / V_{dc})] \quad (11)$$

By using the maximum (I_{max}) and minimum (I_{min}) values of the current wave given in Fig. 3, the transmission losses can be found as in Eqs. (12) and (13).

$$P_{on-h} = [I_o^2 + (I_{max} - I_{min})^2 / 12] \times R_{on-l} \times [1 - (V_o / V_{dc})] \quad (12)$$

$$P_{on-l} = [I_o^2 + (I_{max} - I_{min})^2 / 12] \times R_{on-h} \times [1 - (V_o / V_{in})] \quad (13)$$

Δ_{IL} is ripple current of inductor, f_s is switching frequency, L is inductance value. Ripple current and components is calculated as below.

$$\Delta_{IL} = (V_{dc} - V_o) f_s \times L \times V_o / V_{dc} \quad (14)$$

$$I_{max} = I_o + \Delta_{IL}^2 \quad (15)$$

$$I_{max} = I_o \quad (16)$$

Switching losses is calculated with considering t_{rh} that is high-side MOSFET rise time and t_{fh} that is high-side MOSFET rise time as below:

$$P_{s-h} = 1/2 \times V_{dc} \times I_o \times (t_{rh} + t_{fh}) \times f_s \quad (17)$$

Considering forward direction voltage of low-side MOSFET body diode (V_{di}), low-side MOSFET rise time (t_{rl}) and low-side MOSFET rise time (t_{fl}), P_{s-h} is calculated as:

$$P_{s-l} = 1/2 \times V_{di} \times I_o \times (t_{rh} + t_{fh}) \times f_s \quad (18)$$

Considering the impedance of the coil in direct current (R_{dc}), the inductor current losses are:

$$P_{Lr} = [I_o^2 + (I_{max} - I_{min})^2 / 12] \times R_{dc} \quad (19)$$

I_{CA} is RMS current of capacitor, R_{es} is Equivalent series resistance of capacitor. I_{CA} and P_{CA} can be found with the following equations.

$$P_{CA} = I_o \times (V_{dc} - V_o)^{1/2} \times V_o / V_{dc} \quad (20)$$

$$P_{CA} = I_{CA} (RMS)^2 \times R_{es} \tag{21}$$

The approximate total losses (P_{tl}) can be expressed as follows.

$$P_{tl} = P_{CA} + P_{Lr} + P_{s-l} + P_{s-h} + P_{on-h} + P_{on-l} \tag{22}$$

Considering the output P_o , the total power P_t of the system can be approximated as:

$$P_t = P_o + P_{CA} + P_{Lr} + P_{s-l} + P_{s-h} + P_{on-h} + P_{on-l} \tag{23}$$

3. CIRCUIT APPLICATIONS AND PERFORMANCE

In this section, the performance of the hybrid buck boost converter on R and RL loads is investigated. First, R is driven by a 40V DC source by selecting 5 Ω. The switching time is 0.0001s and the running speed of the simulation is 0.1 ms. The elements used in the circuit and their values are given in Table 1. The PWMs applied to the switches - when the circuit is tested on a 5 Ω load - are given in Fig. 4. In Fig. 4(a), PWMs with operating ratios of 0.5 give a short-term view for better viewing, while in Fig. 4(b), PWMs are shown for full simulation time. Fig. 4(c) shows the DC-DC hybrid converter circuit model applied in MATLAB Simulink.

Table 1. The elements used in the circuit.

Element	Value	Element	Value
R	10 Ω	L2	0.001 H
L	0.0001 H	Vdc1	40 V
C	100 μF	Vdc2	40 V
L1	0.001 H		

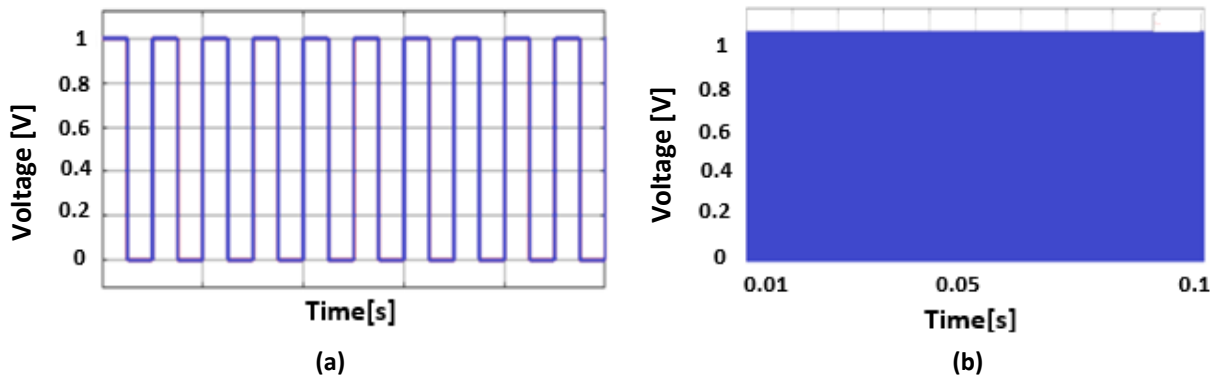
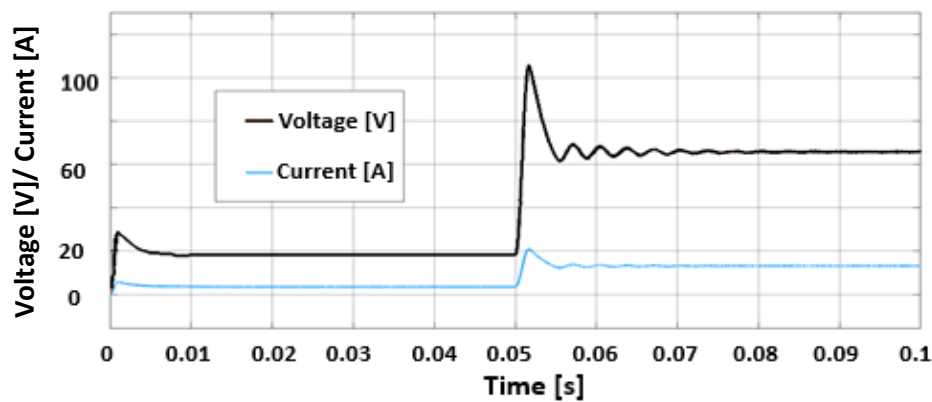


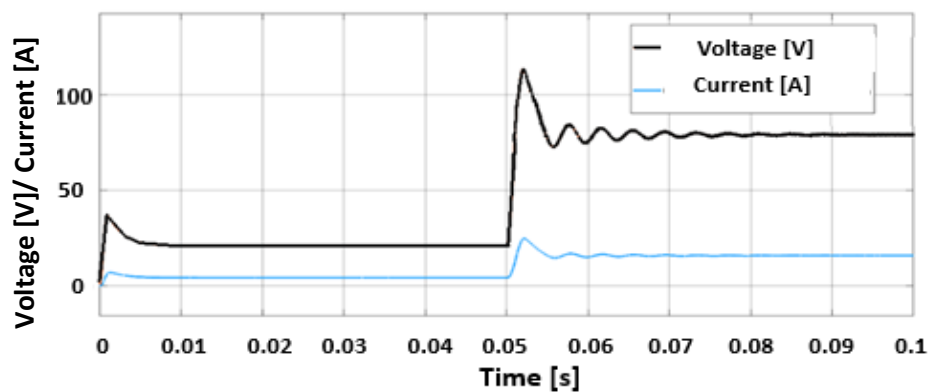
Fig. 4. a) PWM at 0.0001s; b) PWM at 0.1s; c) DC-DC hybrid converter circuit applied in Matlab Simulink.

Firstly, the proposed converter buck and boost modes are tested on the load. The current and voltage on the load are given in Fig. 5(a) when the operating ratio is selected as 0.4 for the converter operating in the mode that decreases in $t_1(0-0.005s)$ time and increases in $t_2(0-0.1s)$ time. The current and voltage on the load are given in Fig. 5(b) after the operating ratio is selected as 0.5 for the converter operating in the mode that decreases in $(0-0.005s)$ of t_1 time and increases in $t_2(0-0.1s)$ time. The current and voltage on the load of 5Ω are given in Fig. 6(a) when the operating ratio is selected as 0.6 for the converter operating in the mode that decreases in $t_1(0-0.005s)$ time and increases in $t_2(0-0.1s)$ time. The current and voltage on the load are given in Fig. 6(b) after the operating ratio is selected as 0.7 for the converter operating in the mode that decreases in $t_1(0-0.005s)$ time and increases between $0s$ and $0.1s$ of t_1 .

When the operating ratio is determined as 0.4, the voltage on the load becomes 16 V. A voltage of 16 V creates a current of 3.2 A over the load. Then, when switching to the increasing mode with the same operating ratio of the switches, the voltage on the load is 66 V and the current is 13.2 A. When the operating ratio is at 0.5, the voltage on the load becomes 20 V. A voltage of 20 V creates a current of 5 A over the load. Then, when switching to the increasing mode with the same operating ratio of the switches, the voltage on the load is 100 V and the current is 20 A. While the operating ratio is 0.6, the voltage on the load becomes 24 V. A voltage of 24 V creates a current of 4.8 A over the load. Then, after switching to the increasing mode with the same operating ratio of the switches, the voltage on the load is 100 V and the current is 20 A.



(a)



(b)

Fig. 5. Buck-boost at: a) 0.4 of D; b) 0.5 of D.

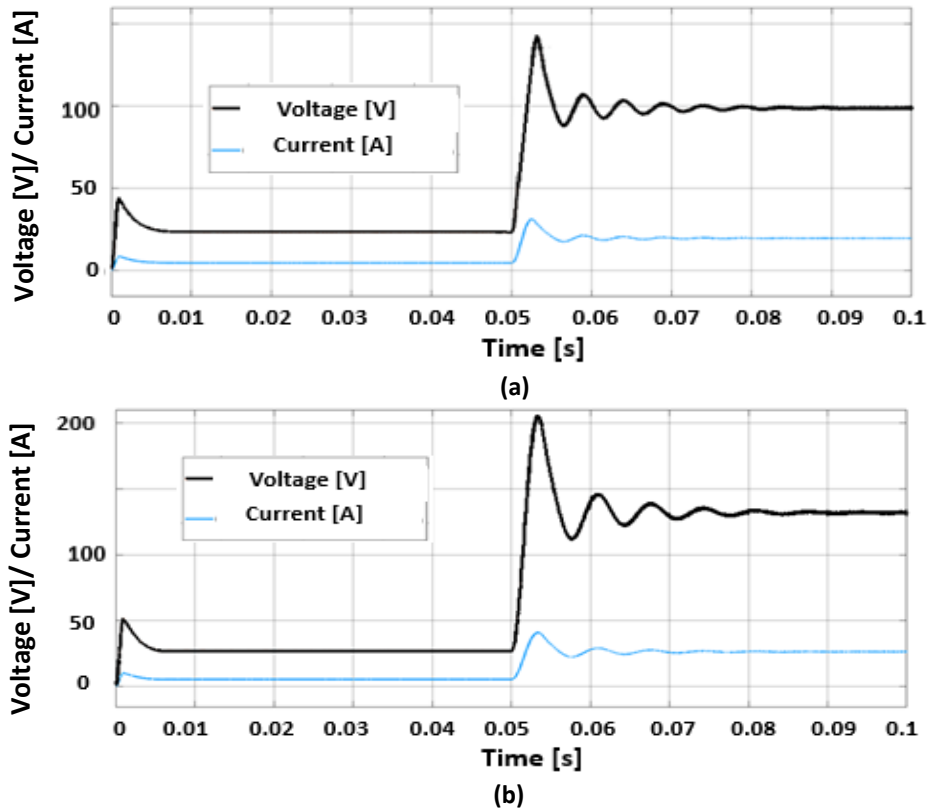
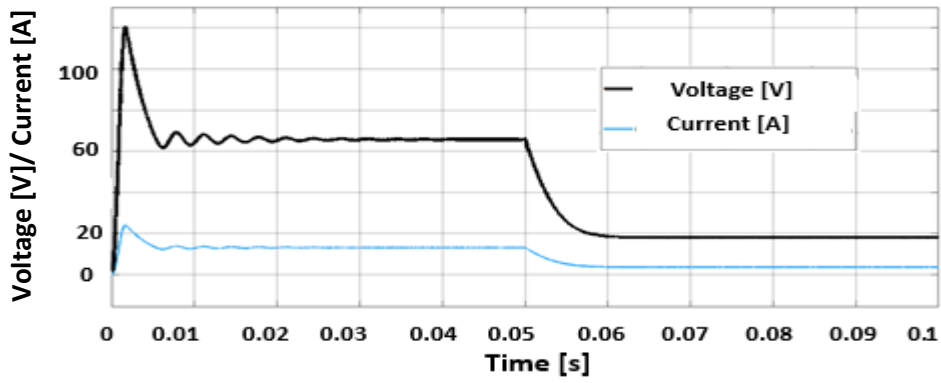


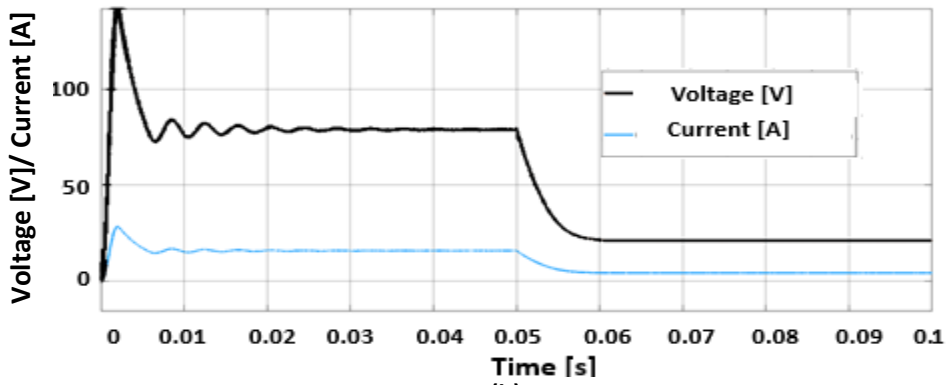
Fig. 6. Buck-boost at: a) 0.6 of D; b) 0.7 of D.

Secondly, the proposed converter first boost and second buck modes are tested on the load. The current and voltage on the load are given in Fig. 7(a) when the operating ratio is selected as 0.4 for the converter operating in the mode that decreases in (0-0.05s) of t_1 time and increases in t_2 (0-0.1s) time. The current and voltage on the load are given in Fig. 7(b) after the operating ratio is selected as 0.5 for the converter operating in the mode that decreases in (0-0.05s) of t_1 time and increases in t_2 (0-0.1) time. The current and voltage on the load of 5Ω are given in Fig. 8(a) when the operating ratio is selected as 0.6 for the converter operating in the mode that decreases between 0s and 0.05s of t_1 and increases between 0s and 0.1s of t_2 time. The current and voltage on the load are given in Fig. 8(b) after the operating ratio is selected as 0.7 for the converter operating in the mode that decreases in (0-0.05s) of t_1 time and increases in (0-0.1s) of t_2 time.

When the operating ratio is determined as 0.4 of D, the voltage on the load becomes 16 V at the 0.05s-0.1s. A voltage of 16 V creates a current of 3.2 A over the load. Then, when switching to the increasing mode with the same operating ratio of the switches, the voltage on the load is 66 V at 0s-0.05s, and the current is 13.2 A. When the operating ratio is at 0.5, the voltage on the load becomes 20 V at 0.05s-0.1s. A voltage of 20 V creates a current of 5 A over the load. Then, when switching to the increasing mode with the same operating ratio of the switches, the voltage on the load is 100 V at the 0-0.05s and the current is 20 A. While the operating ratio is 0.6, the voltage on the load becomes 24 V at 0s-0.05s. A voltage of 24 V creates a current of 4.8 A on the load. Then, after switching to the increasing mode with the same operating ratio of the switches, the voltage on the load is 100 V at 0.05s-0.1s and the current is 20 A. Series connected RL load trials with a resistive load of 5Ω and an inductive load of 0.001H are given in Fig. 9.

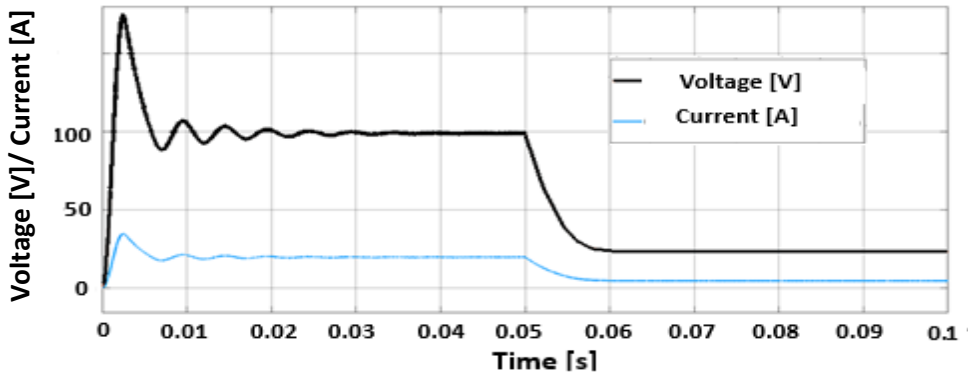


(a)

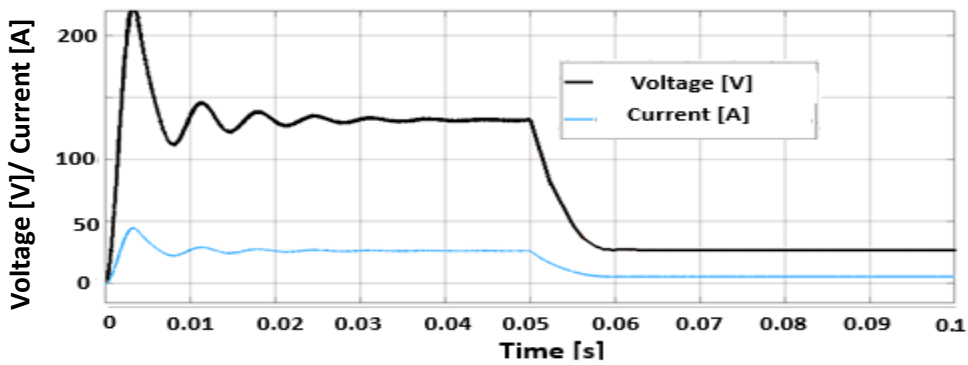


(b)

Fig. 7. Boost and buck at: a) 0.4 of D; b) 0.5 of D.



(a)



(b)

Fig. 8. Boost and buck at: a) 0.6 of D; b) 0.7 of D.

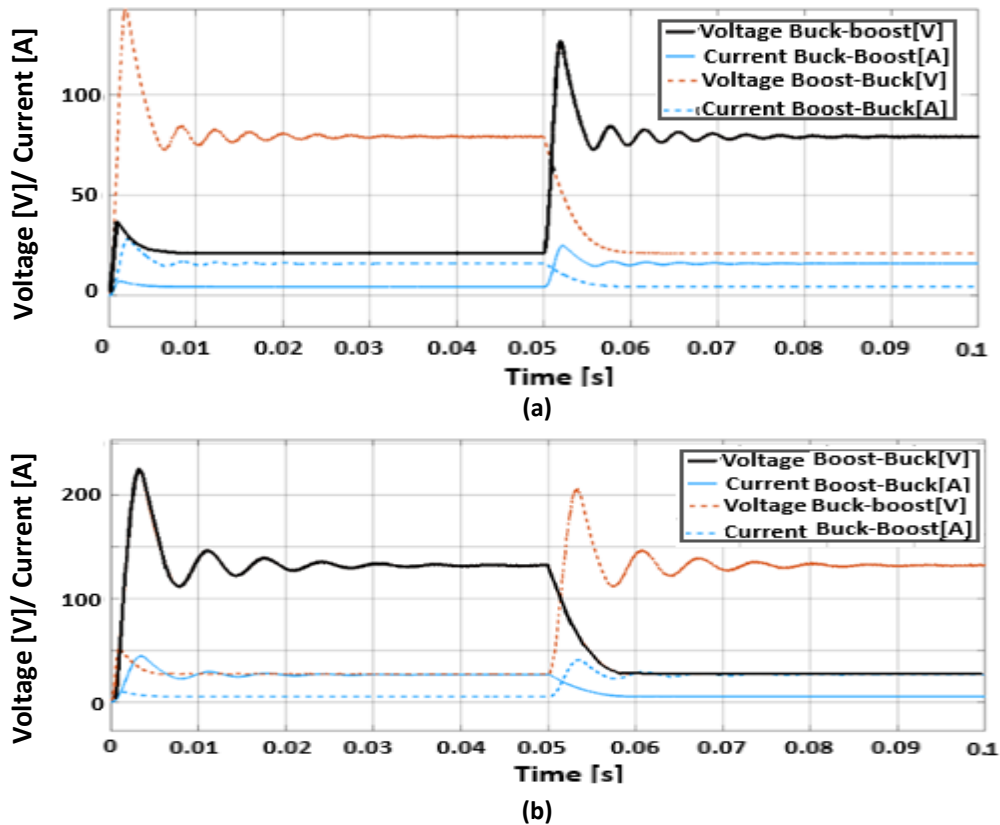


Fig. 9. Converter with series connected RL load at: a) 0.7 of D; b) 0.5 of D.

In order to see the effect of inductive load on the RL load, experiments are carried out by choosing the operating ratio of the switches as 0.7 and 0.5. The inductive load creates a reactance depending on the frequency of the alternating current. It creates negligible impedance in DC current. Therefore, the main factor is the effect of inductivity on the conversion rate. Looking at the obtained results, a voltage of 131 V occurs on the load for 0.7 of operating ratio, and the load current is 26.2 A. In the step-down mode, a load current of 2.38 A occurs against a load voltage of 11.9 V. A voltage of 99 V is on the load for a 0.5 operating ratio, and the load current is 19.8 A. In the step-down mode, a load current of 4.2 A conducts on a load voltage of 21 V. Conventional converters with 40 V and 50 V of the input voltages and the conversion rates on the load of the proposed hybrid converter are given in Table 2. For two DC-DC converter models, the comparison of the power conversion from U_2/R for different resistive load values is given in Table 3.

Table 2. Performance of conventional and the proposed buck-boost converters.

Conventional buck-boost converter		The proposed buck-boost converter			
Input voltage [V]	D	Buck voltage [V]	Boost voltage [V]	Buck-mode voltage [V]	Boost-mode voltage [V]
40	0.4	26	X	16	66 V
40	0.5	40	40	20	80 V
40	0.6	X	60	24	100 V
50	0.4	33.3	X	20	100 V
50	0.5	50	50	20	100 V
50	0.6	X	75	25	125 V

Table 3. Power conversion of conventional and the proposed buck-boost converters for various resistive loads.

Conventional buck-boost converter			The proposed buck-boost converter			
Input Voltage [V]	Load [Ω]	D	Buck Power [W]	Boost Power [W]	Buck-mode Power [W]	Boost- mode Power [W]
40	10	0.4	67.6	X	25.6	435.6
40	10	0.5	160	160	40	640
40	2	0.6	X	180	300	5000
50	2	0.4	554.4	X	200	5000
50	5	0.5	500	500	80	2000
50	5	0.6	X	1125	125	3125

4. ANALYSIS AND DISCUSSION

After the comparison of current and voltage at different loads for the proposed and the conventional converters; the flexibility and advantage of the proposed converter in energy conversion at a fixed modulation index emerge. Then, the differences in power conversion of these two systems are investigated. For two DC-DC converter models, the comparison of the power conversion from U^2/R for different resistive load values is given in Table2. With the proposed converter, a 50 V of input voltage can provide 5000 W of power to the 2 Ω load at 0.4 modulation index for boost mode, while it can provide 200 W of power in buck mode. On the other hand, a conventional DC-DC converter can provide 554.4 W of power to the load under the same conditions. At 40 V of input voltage, the proposed converter can provide 435.6 W of power to a 10 Ω load with a modulation index of 0.4 for the boost mode, while it can provide 25.6 W of power in buck mode. On the other hand, the conventional DC-DC converter can provide a power of 67.4 W to the load under the same conditions. From the results obtained, it turns out that the energy and power conversion provided by the proposed hybrid converter structure is more flexible and have higher ratios than the power conversion provided by conventional converters.

5. CONCLUSIONS

In this article, a common capacitor hybrid buck boost converter is presented. First of all, the operation of the four-stage circuit structure was given together with the working order of the circuit elements. The studies on the circuit R and RL loads were performed by choosing the operating ratios (0.4, 0.5, 0.6 and 0.7) of the switches. The proposed circuit for 0.4 of operating ratio produced 16 V in buck mode and 100 V in boost mode, while the conventional buck-boost converter generated only 26 V. The hybrid buck boost converter for 0.5 operating ratio produced 20 V in buck mode and 80 V in the boost mode, while the conventional buck-boost converter generated only a constant 50 V. The proposed circuit for 0.6 operating ratio produced 24 V in buck mode and 80 V in boost mode, while conventional buck-boost converter generated only 60 V. The aforesaid obtained results show that the proposed hybrid converter - compared the conventional ones - can produce more effectively different output values for the same operating ratios.

REFERENCES

- [1] E. Muljadi, J. Bialasiewicz, "Hybrid power system with a controlled energy storage," *In 29th Annual Conference of the IEEE Industrial Electronics Society*, vol. 2, pp. 1296-1301, 2003.
- [2] E. Muljadi, H. Mckenna, "Power quality issues in a hybrid power system," *In Conference Record of the 2001 IEEE Industry Applications Conference, 36th IAS Annual Meeting*, vol. 2, pp. 773-781, 2001.
- [3] F. Valenciaga, P. Puleston, "Supervisor control for a stand-alone hybrid generation system using wind and photovoltaic energy," *IEEE Transactions on Energy Conversion*, vol. 20, no. 2, pp. 398-405, 2005.
- [4] S. Sivakumar, M. Sathik, P. Manoj, G. Sundararajan, "An assessment on performance of DC-DC converters for renewable energy applications," *Renewable and Sustainable Energy Reviews*, vol. 58, pp. 1475-1485, 2016.
- [5] S. Danyali, A. Moradkhani, R. Aazami, M. Mejbil, "New dual-source high-gain ZVS DC-DC converter for integrating renewable power source and battery storage," *Electric Power Systems Research*, vol. 213, pp. 108740, 2022.
- [6] A. Deihimi, M. Mahmoodieh, "Analysis and control of battery-integrated dc/dc converters for renewable energy applications," *IET Power Electronics*, vol. 10, no. 14, pp. 1819-1831, 2017.
- [7] A. Sadhukhan, P. Gayen, S. Saha, "High performance of dual input H-bridge DC-DC converter in solar application," *AEU-International Journal of Electronics and Communications*, vol. 154, pp. 154295, 2022.
- [8] M. Choudhary, M. Saqi, M. Javed, H. Gelani, M. Akram, M. Amjad, S. Khan, "Solar powered space vector pulse width modulation based induction motor drive for industry applications," *Bulletin of Electrical Engineering and Informatics*, vol. 11, no. 4, pp. 1828-1836, 2022.
- [9] J. Cai, X. Zhang, W. Zhang, Y. Zeng, "An integrated power converter-based brushless DC motor drive system," *IEEE Transactions on Power Electronics*, vol. 37, no. 7, pp. 8322-8332, 2022.
- [10] E. Can, H. Sayan, "The performance of the DC motor by the PID controlling PWM DC-DC boost converter," *Tehnički Glasnik*, vol. 11, no. 4, pp. 182-187, 2017.
- [11] N. Dias, A. Naik, "Design, modeling and simulation of bidirectional buck and boost converter for electric vehicles," *In 2022 International Conference for Advancement in Technology*, pp. 1-5, 2022.
- [12] S. Desingu, A. Mouttou, "Control of improved non-isolated high gain DC-DC converter," *Jordan Journal of Electrical Engineering*, vol. 7, no. 1, pp. 43-58, 2021.
- [13] Y. Ashraf, N. Elsobky, M. Hamouda, M. Sabry, S. Kaddah, B. Badr, "Controlling single-stage and quasi-resonant flyback converters for solar power systems," *Jordan Journal of Electrical Engineering*, vol. 7, no. 2, pp. 148-165, 2021.
- [14] O. Ibrahim, N. Yahaya, N. Saad, "Phase-shifted full-bridge zero voltage switching DC-DC converter design with MATLAB/Simulink implementation," *International Journal of Electrical and Computer Engineering*, vol. 8, no. 3, pp. 1488, 2018.
- [15] M. Banaei, H. Bonab, "A high efficiency nonisolated buck-boost converter based on ZETA converter," *IEEE Transactions on Industrial Electronics*, vol. 67, no. 3, pp. 1991-1998, 2019.
- [16] M. Gaboriault, A. Notman, "A high efficiency, noninverting, buck-boost DC-DC converter," *In Nineteenth Annual IEEE Applied Power Electronics Conference and Exposition*, vol. 3, pp. 1411-1415, 2004.
- [17] A. Rajabi, F. Shahir, R. Sedaghati, "New unidirectional step-up DC-DC converter for fuel-cell vehicle: design and implementation," *Electric Power Systems Research*, vol. 212, pp. 108653, 2022.
- [18] R. Uthirasamy, V. Chinnaiyan, S. Vishnukumar, A. Karthick, V. Mohanavel, U. Subramaniam, M. Muhibbullah, "Design of boosted multilevel DC-DC converter for solar photovoltaic system," *International Journal of Photoenergy*, vol. 2022, 2022.

- [19] A. Rajabi, A. Rajaei, V. Tehrani, P. Dehghanian, J. Guerrero, B. Khan, "A non-isolated high step-up DC-DC converter using voltage lift technique: analysis, design, and implementation," *IEEE Access*, vol. 10, pp. 6338-6347, 2022.
- [20] D. Graovac, M. Purschel, A. Kiep, "MOSFET power losses calculation using the data-sheet Parameters," *Infineon Application Note*, vol. 1, pp. 1-23, 2006.
- [21] S. Wong, A. Brown, Y. Lee, S. Ng, "Parasitic losses modeling of a series resonant converter circuit," *In Proceedings of the 1997 IEEE International Symposium on Circuits and Systems*, vol. 2, pp. 921-924, 1997.